

more GaAs to be sputtered away. This effect has been quantified by an AFM image taken after the gates and sidewalls have been removed. Multiple lines of a 3D AFM image were averaged to obtain the sectional image of Fig. 2. With a 600nm thick SiO₂ film and a 10% over etch, a trench depth of 21nm is observed, compared to ≈ 11nm of GaAs removed by the combined refractory gate and sidewall etches in the field region. The SiO₂ etch rate is 19nm/min compared to a GaAs sputter rate of 2nm/min in the RIE using CHF₃/O₂ chemistry. SEM images have not been suitable for quantifying GaAs sputter removal owing to resolution limitations, nor has this effect been reported previously.

Because this GaAs sputtering can be detrimental to shallow-channel devices, we have investigated methods for eliminating this effect. The trench could be reduced either by reducing the GaAs exposure to the plasma, or reducing the sputter rate of the GaAs in the plasma. The latter is not a viable approach since sputtering is unavoidable owing to the requirement for anisotropy. To achieve the former, the selectivity of the sidewall etch against GaAs can be increased, or the cusp in the dielectric film can be eliminated. We succeeded in increasing the selectivity by switching to a Si₃N₄ PECVD film and using a SF₆/CHF₃ chemistry, thereby increasing the Si₃N₄ etch rate to 83nm/min. As this chemistry also increased the GaAs sputter rate to 9nm/min, no net increase in selectivity resulted. A 2-step etch using the SF₆/CHF₃ chemistry for the majority of the etch and CHF₃/O₂ chemistry (with a comparable Si₃N₄ etch rate) near endpoint and during the over etch period resulted in a selectivity increase which was more than four-fold, and virtual elimination of the trench. This is shown in the AFM sectional image of Fig. 3. The total GaAs removal, which includes the gate etch as well as the sidewall etch, has been reduced to 6nm. No FET results are yet available to quantify the effect of the trench, but negative effects on source resistance and short-channel characteristics are expected.

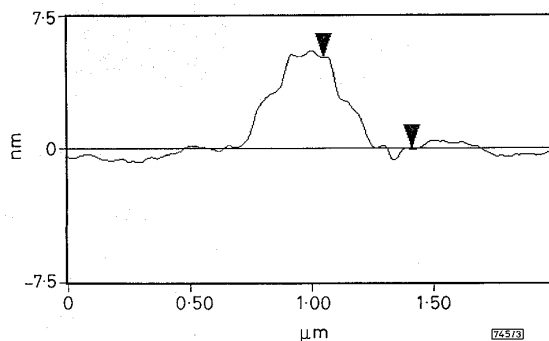


Fig. 3 AFM section analysis of gate region after sidewalls and gates have been removed following Si₃N₄ sidewall etching with a 2-step etch chemistry

Trench has been eliminated and GaAs sputtering has been greatly reduced

Conclusion: GaAs trenches ~21nm deep have been observed as a result of a commonly employed sidewall process used for self-aligned GaAs FETs. This trench derived from a cusp in the dielectric deposition over W-based gates as well as a slow SiO₂ etch rate compared to the GaAs sputter rate. The trench is eliminated by using a higher etch rate dielectric, Si₃N₄, and a two-step etch chemistry. These results are of potential significance in the design and performance of shallow channel GaAs FETs.

Acknowledgments: The authors would like to thank A. T. Ongstad and L. Griego for their technical support. This work was performed at Sandia National Laboratories supported by the U.S. Department of Energy under contract No. DE-AC04-94AL85000.

© IEE 1996

4 September 1995

Electronics Letters Online No: 19960017

A.G. Baca, A.J. Howard, R.J. Shul and M.E. Sherwin (Sandia National Laboratories, Albuquerque, NM 87185-0603, USA)

References

- ASAI, S., GOTO, N., KANAMORI, M., TANAKA, Y., and FURUTSUKA, T.: 'A high performance LDD GaAs MESFET with a refractory metal gate'. Extended abstracts 18th Conf. Solid State Devices and Materials, 1986, pp. 383-386
- BOISSENOT, P., DELHAYE, E., MALUENDA, J., FRIJLINK, P., VARIN, C., DESCHAMPS, F., and LECURU, I.: 'A 0.4µm gate-length AlGaAs/GaAs p-channel HIGFET with 127mS/mm transconductance at 77K', *IEEE Electron Device Lett.*, 1990, **EDL-11**, pp. 282-284
- HIDA, H., TSUKADA, Y., OGAWA, Y., TOYOSHIMA, H., FUJII, M., SHIBAHARA, K., KOHNO, M., and NOZAKI, T.: 'Novel self-aligned gate process technology for i-AlGaAs/n-GaAs doped-channel hetero-MISFET(DMT) LSIs based on E/D logic gates'. IEDM Tech. Dig., 1988, pp. 688-691
- HIGASHISAKA, A., ISHIKAWA, M., KATANO, F., ASAI, S., FURUTSUKA, T., and TAKAYAMA, Y.: 'Sidewall-assisted closely spaced electrode technology for high speed GaAs LSIs'. Extended abstracts 15th Conf. Solid State Devices and Materials, 1983, pp. 69-72
- TSUNOTANI, M., YAMAMOTO, N., KIMURA, T., INOKUCHI, K., and SANO, Y.: 'Advanced self-alignment process technique with very thick sidewall for high speed GaAs LSIs'. IEDM Tech. Dig., 1988, pp. 700-703
- UENO, K., FURUTSUKA, T., TOYOSHIMA, H., KANAMORI, M., and HIGASHISAKA, A.: 'A high transconductance GaAs MESFET with reduced short channel effect characteristics'. IEDM Tech. Dig., 1985, pp. 82-85
- KIEHL, R.A., HALLALI, P.E., YATES, J., TISCHLER, M.A., POTEMSKI, R.M., and CARDONE, F.: 'High-transconductance p-channel AlGaAs/GaAs HFETs with low-energy beryllium and fluorine co-implantation self-alignment', *IEEE Electron Device Lett.*, 1991, **EDL-12**, pp. 530-532
- SHUL, R.J., RIEGER, D.J., BACA, A.G., CONSTANTINE, C., and BARRATT, C.: 'Anisotropic electron cyclotron etching of tungsten films on GaAs', *Electron. Lett.*, 1994, **30**, pp. 84-85
- KANAMORI, M., NAGAI, K., and NOZAKI, T.: 'Low-resistivity W/WSi_x bilayer gates for self-aligned GaAs metal-semiconductor field-effect transistor large-scale integrated circuits', *J. Vac. Sci. Technol.*, 1987, **B5**, pp. 1317-1320

Evolutionary linearisation in the frequency domain

Kay Chen Tan, Ming Rui Gong and Yun Li

Indexing terms: Nonlinear systems, Linearisation techniques

Few solutions have been found so far to frequency domain MIMO system linearisation problems owing to practical difficulties in obtaining derivatives of the nonlinear model. The authors develop an evolutionary linearisation technique to achieve an automated linearisation goal, directly using the plant I/O data. It allows linearisation for an entire operating region and for the entire interested frequency range, the benefits of which cannot be matched by existing methods.

Introduction: Almost all engineering systems (or plants) are nonlinear in practice. To design a control system for a nonlinear plant, both classical and modern control theories usually require a linearised nominal model of the plant. Linearisation of a nonlinear system is often carried out using a calculus based Taylor expansion around an equilibrium operating point. Such a method is only valid if the nonlinearity of the plant is differentiable in engineering practice. It becomes much more difficult when the plant is a multiple-input and multiple-output (MIMO) system. This linearisation method may only be suitable if the plant operates in a relatively very small or very linear region, the condition of which can often not be satisfied by the variable amplitude control signal. Further, this method of linearisation may result in the loss of some frequency response characteristics of the original system [1], which are important to frequency domain based control system design methods. Thus, in this Letter, an automated multivariable system linearisation technique based on system input-output behaviour is developed.

Problem formulation: A laboratory test-rig that simulates liquid-level regulation systems such as those widely found in chemical or dairy plants is experimented upon in this Letter. It is a coupled nonlinear system as described by the state-space equations

$$\begin{bmatrix} \dot{h}_1 \\ \dot{h}_2 \end{bmatrix} = \begin{bmatrix} -\frac{C_1 a_1}{A} \sqrt{2g(h_1 - h_2)} \\ \frac{C_1 a_1}{A} \sqrt{2g(h_1 - h_2)} - \frac{C_2 a_2}{A} \sqrt{2g(h_2 - H_3)} \end{bmatrix} + \begin{bmatrix} \frac{1}{A} & 0 \\ 0 & \frac{1}{A} \end{bmatrix} \begin{bmatrix} q_1 \\ q_2 \end{bmatrix} \quad (1)$$

Here, h_1 and h_2 are the liquid levels of tank 1 and tank 2, respectively; q_1 and q_2 are input flow rates mapped from the pump voltages; $C_1 = 0.53$ and $C_2 = 0.63$ are discharge constants; $a_1 = 0.396\text{cm}^2$ and $a_2 = 0.385\text{cm}^2$ are orifice areas; $A = 100\text{cm}^2$ is the cross-sectional area of both tanks; and $g = 981\text{cm/sec}^2$ is the gravitational constant. There is a practical constraint imposed on this system by its physical structure, i.e. $H_3 = 3\text{cm}$, the minimum liquid level bounded by the height of the orifices.

If this two-input and two-output nonlinear system can be linearised, a transfer function matrix model given by

$$\hat{G}(s) = \begin{bmatrix} \hat{G}_{11}(s) & \hat{G}_{12}(s) \\ \hat{G}_{21}(s) & \hat{G}_{22}(s) \end{bmatrix} \quad (2)$$

may be used to describe the linearised system, where $i, j \in \{1, 2\}$ and every transfer function element is of the form

$$\hat{G}_{ij}(s) = \frac{b_m s^m + b_{m-1} s^{m-1} + \dots + b_0}{s^n + a_{n-1} s^{n-1} + \dots + a_0} \quad (3)$$

It is noted that the denominators of all $G_{ij}(s)$ should be the same, determining the characteristics or the poles of the linearised system.

To assess how accurately the linearised model performs in the frequency domain, an error norm is usually used. Let L_x represent the L_1 , L_2 and L_∞ norms in the Euclidean space for $x = 1, 2$ and ∞ , respectively. This norm can further be weighted as given by

$$\begin{aligned} J_{i,j} &= \left\| W(j\omega) \left[\hat{G}_{i,j}(j\omega) - G_{i,j}(j\omega) \right] \right\|_x \\ &= \sqrt[N]{\sum_{k=1}^N |W(j\omega_k) \left[\hat{G}_{i,j}(j\omega_k) - G_{i,j}(j\omega_k) \right]|^x} \end{aligned} \quad (4)$$

where $G_{ij}(j\omega_k)$ represents the 'frequency response' data of the nonlinear system under the operating condition concerned; $W(j\omega)$ is the weighting function that allows fitting errors in some chosen parts of the frequency range to have particular emphasis; and N is the number of data points used.

Given a pre-specified order required on the linearised model, the objective here is thus to obtain an optimal $\hat{G}(s)$ of multiple parameters that results in the minimum linearisation error as defined by

$$J = \sum_{j=1}^2 \sum_{i=1}^2 J_{i,j} \quad (5)$$

If it is required, however, the diagonal and non-diagonal elements may be weighted distinctively. The complexity in obtaining solutions to multimodal problems like this has presented the use of analytical and conventional numerical means [2]. Attempts at solving this important problem have thus been unsuccessful so far.

Evolutionary linearisation: One possible way to obtain numerical solutions to such MIMO system linearisation problems would be to exhaustively search for an optimal answer. This is, however, practically impossible, as an enumerative algorithm requires exponential, as opposed to polynomial, search time and will thus easily break down owing to the high parametric dimensionality of this type of problem. In contrast, the evolutionary algorithm (EA) [2] is a polynomial algorithm that improves tractability and robustness in global optimisations by slightly trading off precision in a nondeterministic manner. Such an algorithm can 'intelligently' explore, without the need of a differentiable or well behaved performance index, a noisy and poorly understood space at multiple points by a population of candidate solutions leading to several globally optimised answers.

A basic EA involves three types of operation, namely, selection crossover, (or recombination of parameters), and mutation. In an ordinary EA such as a genetic algorithm (GA), however, the mutation rate is low to avoid the evolution becoming a useless

random search. Conversely, this may result in the 'stagnation problem' when the population evolves to become more homogeneous. Further, a standard GA lacks ability in local exploitation and thus in finding closer optima at each level of search [2]. Therefore, in this Letter, the mutation is realised by multi-point simulated annealing (SA) to achieve a more accurate search and a faster convergence. A similar SA enhanced evolutionary algorithm has been successfully applied to solve time domain linearisation problems [3].

Without loss of generality, consider the nonlinear system of eqn. 1 to be linearised to a causal second-order model given by eqn. 2 and eqn. 3 with $n = 2$ and $m \leq 1$. To reflect practical applications as discussed in the introduction, the linearised model will provide the best fit for a pre-specified operating region around the operating point. This means two DC voltages are first applied to set the steady-state operating (and equilibrium) points and then two bipolar AC voltages with, for example, $\pm 5\%$ amplitude relative to the set voltages, are applied. The values of the interested frequency range can be used to determine the 'clock' that generates pseudo random binary sequences (PRBS) such that the PRBS signals can act as additive excitations mainly covering the interested frequency points.

Based on this scheme, studying eqn. 4 again leads to the strategy of using a PRBS signal as the weighting function, as well as the input function. Thus, in eqns. 4 and 5, the task of minimising the errors of transfer is reduced to the task of minimising the output errors. In this study, the interested frequency ranges from 4×10^{-3} to 4×10^{-2} rad/s, as the plant is relatively sluggish. In the laboratory simulations, the operating point of tank 1 is set at 10cm and that of tank 2 at 8cm using step input voltages. By holding the input to tank 2 constant, the PRBS signal is added to input 1 and both outputs are collected for evaluating $W_1(j\omega)G_{11}(j\omega)$ and $W_1(j\omega)G_{21}(j\omega)$. This procedure is repeated for input 2.

In the evolutionary linearisation program, different candidate parameter sets of the linear models in the population result in different $G_{ij}(j\omega_k)$ with different linearisation quality. Without loss of generality, the quality of fitting is measured in this Letter by the L_2 norm, as all L_x norms are finite bounded with one another (i.e. metric equivalence). To minimise this norm, a similar EA to that of [3] is enhanced by Monte Carlo mutation with a hyperbolic tangent distribution, using the Boltzmann selection rule. This linearisation program was executed to evolve for 150 generations of 100 candidate solutions to eqn. 5. The best linearised second-order model obtained at the end of the evolutions is given by

$$G(s) = \frac{1}{\Delta} \begin{bmatrix} 4.1041s + 0.7688 & 0.4805 \\ 0.4945 & 5.3153s + 0.5305 \end{bmatrix} \quad (6)$$

where

$$\Delta = s^2 + 49.05s + 0.5385 \quad (7)$$

The frequency response of this linear model is depicted by the dotted lines in Fig. 1.

Validation: To validate the linearised model, time domain simulations on the differential equations given by eqn. 1 have been performed, using the fourth-order Runge-Kutta numerical integration method. Similar procedures are used to acquire the frequency response data of the cross transfers in the nonlinear MIMO system. Here both output and input data are collected for a longer period of time than before. Then these data are converted to spectra using fast Fourier transforms for the frequency range 3×10^{-3} rad/s to 5.5×10^{-2} rad/s, over-covering the points of interest. By dividing the magnitudes of the output spectra with those of the corresponding input, the gains of the point-linearised system are obtained. The phases of the system can also be obtained by subtracting the phases of the output from those of the inputs. These are depicted by the solid lines in Fig. 1. For a better comparison, the frequency responses of the linearised model are also plotted for the augmented range to study how accurate the fitting is outside the linearising frequency range. It can be seen that both magnitude and phase are fitted very accurately, although the minimisation objective given by eqns. 4 eqn. 5 is mainly focused on magnitude.

Conclusions: In this Letter, evolutionary linearisation techniques have been developed to solve frequency domain system linearisation problems that have had few solutions to date. The method

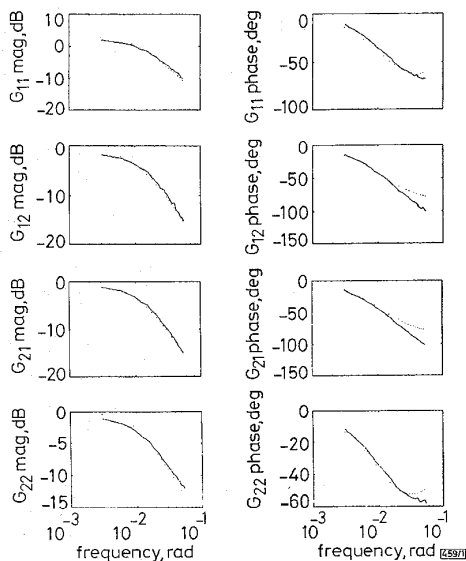


Fig. 1 Frequency responses of linearised (---) and original (—) system

uses the plant I/O data directly and requires no derivatives, which cannot often be obtained from a practical nonlinear MIMO system. Further, this method allows linearisation for an entire operating region and for the entire interested frequency range. Such benefits cannot be matched by existing methods.

Acknowledgments: Kay Chen Tan and Ming Rui Gong are grateful to the University of Glasgow, CVCP and EPSRC for their financial support.

© IEE 1996

13 November 1995

Electronics Letters Online No: 19960061

Kay Chen Tan, Ming Rui Gong and Yun Li (Department of Electronics and Electrical Engineering, University of Glasgow, Glasgow G12 8LT, United Kingdom)

References

- FRANKLIN, G.F., POWELL, J.D., and EMAMI-NAENINI, A.: 'Feedback control of dynamic systems' (Addison-Wesley, 1991)
- RENDERS, J.M., and BERSINI, H.: 'Hybridising evolution algorithms with hill-climbing methods for global optimisation: Two possible ways'. Proc 1st IEEE Int. Conf. Evolutionary Computing, IEEE World Cong. Comp. Intel., Orlando, 1994, 1, pp. 312-317
- TAN, K.C., LI, Y., MURRAY-SMITH, D.J., and SHARMAN, K.C.: 'System identification and linearisation using evolution algorithms with simulated annealing'. Proc. 1st IEE/IEEE Int. Conf. Genetic Algorithms in Eng. Syst.: Innovations and Appl., Sheffield, United Kingdom, 1995, pp. 164-169

System identification via singular value decomposition

Shih-Ho Wang, T.F. Lee and R. Zachery

Indexing terms: Singular value decomposition, Optimisation

The problem of identifying linear time invariant system parameters from their truncated impulse response data is studied. The authors analyse the algorithm originally proposed by Kung, and later modified by others, which is based on the singular value decomposition of the Hankel matrix. They propose a modified algorithm which generates more accurate results.

Introduction: In this Letter, we study the problem of identification of system parameters from their truncated impulse response data.

In [1] Kung has proposed an algorithm that is based on the singular value decomposition of the Hankel matrix. In [2] this algorithm, and a new version of it, have been studied.

We will show that there are some unintended weighting factors in the error function to be minimised by these algorithms. We propose introducing a parameter in the computation to reduce the effect of the unintended weighting factors. We demonstrate our method by producing more accurate results using example in [1, 2].

Problem formulation: Following the notation in [2], consider a linear time invariant system described by the following minimal state space representation:

$$x(k+1) = Ax(k) + bu(k) \quad (1)$$

$$y(k) = cx(k) \quad (2)$$

where $A \in R^{p \times p}$, $b \in R^{p \times 1}$ and $c \in R^{1 \times p}$. The impulse response of this system is

$$h(k) = cA^{k-1}b \quad k = 1, 2, 3, \dots \quad (3)$$

The system identification problem is as follows: given the first $(2n - 1)$ terms of the impulse response, find the system matrices A , b and c . The Kung algorithm proceeds as follows: form the following $n \times n$ Hankel matrix,

$$H = \begin{bmatrix} h(1) & h(2) & \dots & h(n) \\ h(2) & h(3) & \dots & h(n+1) \\ \dots & \dots & \dots & \dots \\ h(n) & h(n+1) & \dots & h(2n-1) \end{bmatrix} \quad (4)$$

Then compute the singular value decomposition of H

$$H = USV^T \quad (5)$$

where U and V are $n \times n$ orthogonal matrices, and S is an $n \times n$ diagonal matrix of the singular values of H , i.e.

$$S = \text{diag}(s_1, s_2, \dots, s_n) \quad (6)$$

If the system is of the order p , then the first p singular values of S are significantly larger than the rest. By examining the singular values, choose the system order p and then generate the system matrices (A, b, c) based on U, V and s_1, s_2, \dots, s_p . The details are omitted here.

In [2], a modified version of Kung's algorithm is given. The main difference is that the H matrix is defined as

$$H = \begin{bmatrix} h(1) & h(2) & \dots & h(N) \\ h(2) & h(3) & \dots & 0 \\ \dots & \dots & \dots & \dots \\ h(N) & 0 & \dots & 0 \end{bmatrix} \quad (7)$$

where $h(1), \dots, h(N)$ are the given impulse response data. Notice that in this modified H matrix, N could be an even or an odd number, although in [2], N was chosen as $2n - 1$.

The rest of the modified algorithm is essentially the same as the original Kung algorithm.

Error analysis: The exact error function associated with the above algorithm is very complex. However, the result of the above algorithm can be viewed as an approximate solution to the following optimisation problem:

We consider the modified Kung algorithm. Given a Hankel matrix H of size $N \times N$, find another Hankel matrix H' of rank p , where p is $< N$, such that the following error function is minimised:

$$\|H - H'\|_F$$

where $\|\cdot\|_F$ is the Frobenius norm. Let $h'(i+j-1)$ be the element in the i -th row and the j -th column of the H' matrix. Define

$$e(i) = h(i) - h'(i) \quad i = 1, \dots, N$$

and

$$e(i) = -h'(i) \quad i = N+1, \dots, 2N-1$$

Hence the error function can be written as a function of $e(i)$ as follows:

$$d(e(1), e(2), \dots, e(2N-1)) = \|H - H'\|_F \quad (8)$$

For small $e(i)$, $d(\cdot)$ can be approximated as